

## Distribution Relationship Between Veins of Groundwater, Slope angles, and Slope Failures at a Landslide in Crystalline Schist Area

Gen FURUYA\*, Kyoji SASSA, Akira SUEMINE

\* COE Researcher, DPRI, Kyoto University

### Synopsis

The present study is concerned with the assessment of the distribution of the potential considered about the location of slope failures in a crystalline schist area triggered by heavy rainfall based on the results of one-meter depth underground temperature survey, slope stability, and water quality analysis. The slope failures appear to concentrate around the vein of groundwater and the veins of groundwater rising from deep layers. There are two types of groundwater from origination the deep layers, one is short storage time the other is long storage time. By combining the results of stability analysis and distribution of veins of groundwater, it is suggested that the localization of zones of high potential for slope failure can be narrowed down to some extent.

**Keywords:** heavy rainfall, distribution of slope failures, one-meter depth underground temperature survey, stability analysis, water quality analysis

### 1. Introduction

Most of the slope failures in Japan are caused by heavy rainfall. In some cases, slope failure mass may generate fluidized landslides (debris flows), which could cause serious disasters every year. Many slope failures took place in Zentoku, Nishi-iyayama village, Tokushima Prefecture due to 29 June 1999 the heavy rainfall correspond to a probability of occurrence of 1/80 – 1/100 years (Hiramatsu et al., 1999). Some of the slope failures turned into debris flows, causing serious damage to houses and roads.

Numerous field examinations of the areas of slope failure have been done until now. According to statistical interpretation of the slope angle of high potential of slope failure in Japan by Kaibori (1986), the slope with gradients ranging 30° to 60° shows the highest frequency of failure. It was pointed out that the location of potential slope failure was the lower slope at knick point and 0-order basin (e.g. Tsukamoto et al., 1973). Okimura et al. (1988, 1989)

examined the slope failure occurrence by means of geomorphologic and soil mechanical properties in Granite mountainous areas. It was found that 1) most effective factors of decreasing safety factor were slope angle and depth of sliding mass, 2) 30% of the investigation area showed high potential of slope failure as calculated from their simulation. However, even for a heavy rainfall occurring once at 10 years, the number of slope failures was unusually in excess of 10% in a watershed (Tanaka, 1985).

It is well known that the dominant factor associated with slope failures during a heavy rainfall is the increasing of pore water pressure. Therefore, the precise knowledge of this parameter is necessary to clarify the mechanism of slope failure during a heavy rainfall. Generally, groundwater is assumed uniform when the mechanism of slope failure is examined. On the other hand, Takeuchi (1981) pointed out that the groundwater of natural slope is vein-like flowing. Consequently, if the vein of groundwater that generates pore water pressure is

grasped plane, the location of slope failure may be able to be narrowed down to some extent. However, the relationship between the veins of groundwater distribution and the location of slope failure isn't yet clarified.

In this study, we carry out the one-meter depth underground temperature survey and the stability analysis at every grating slope to clarify the relationship between the distribution of slope failures and veins of groundwater at a landslide in crystalline schist area. Furthermore, the water quality was investigated at the springs and boreholes in and around study area to clearly approximate the supplying depth of groundwater related to slope failures.

## 2. Brief view of study area

Fig. 1 shows location of the Zentoku area. The Zentoku area locates in the crystalline schist area in

the middle of Shikoku Island, southwestern Japan. The investigation was carried out at the B, C tributary, Tobinosu torrent and the Taishi-do area that locates of at the middle slope of Zentoku area. The middle and lower part of the bedrock in Zentoku area consists mainly of pelitic and partially green schist. The lower part of the slope is comprised of psammitic schist. Furuya et al., (1999) pointed out that the slip surface of the Z6 block has formed at depths of 30-60m as shown in Fig. 2. On the other hand, the Tobinosu torrent has not reported landslide movement such as the Z6 block. However, weathered material and colluvium can be found at depths of 1-3m, and the bedrock and large rocks are locally exposed.

Fig.3 shows the topography of the Taishi-do area. The average slope angle of the Taishi-do area is 32°. There are four slope failures caused by the heavy rainfall at the Taishi-do area. In the largest slope failure (called slope failure at Taishi-do), the

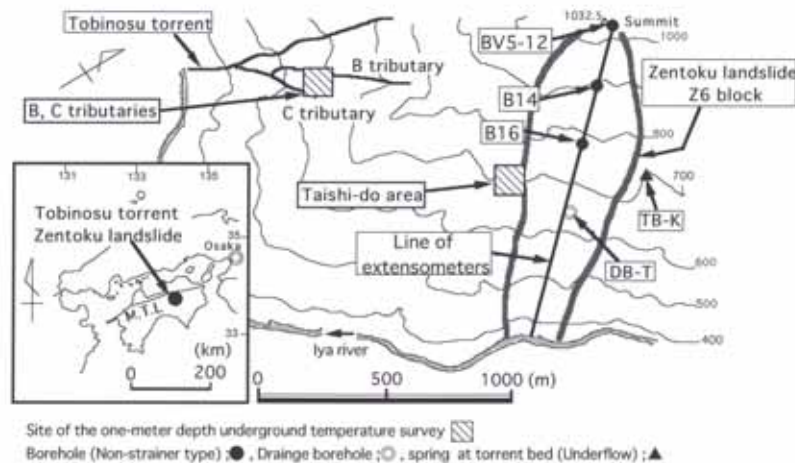


Fig. 1 Location map of investigation area in the Zentoku landslide

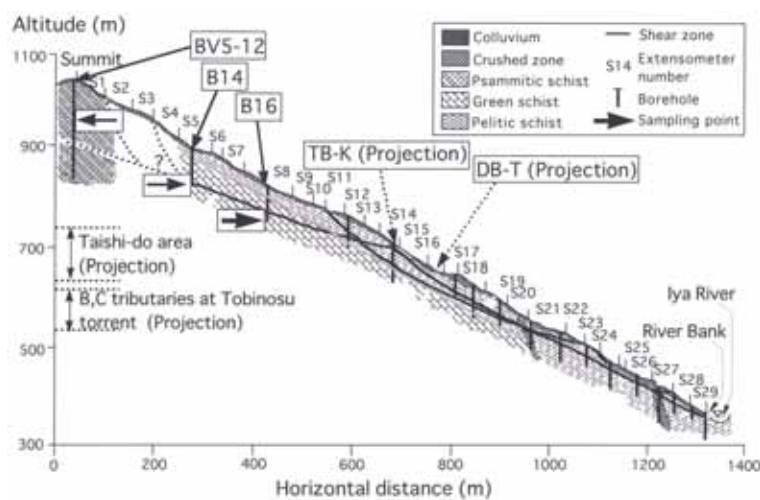


Fig. 2 Cross-section through the Zentoku landslide along the line of extensometers and location of measurement points of groundwater temperature

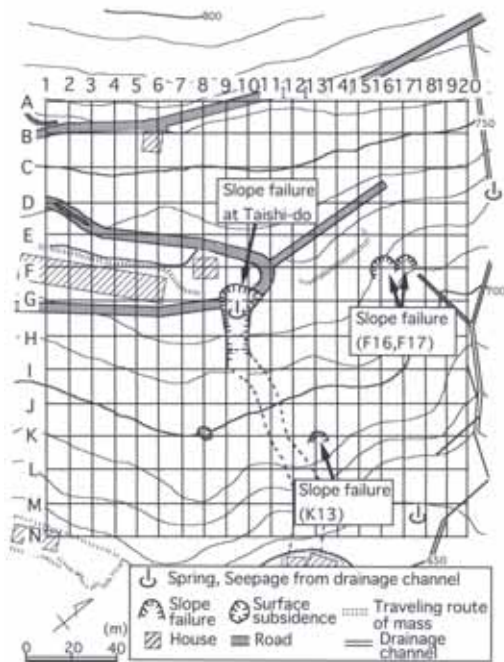


Fig. 3 Measurement net of the Taishi-do area

depth of slip surface is 3m and volume is approximately 500m<sup>3</sup>(Furuya et al., 2000). For the other slope failures, the depth of slip surface is within 1-2m and volume is approximately 100m<sup>3</sup>. There are three springs at the Taishi-do area located at the bottom of the failed slope at Taishi-do, approximately 140m east side of the slope failure at Taishi-do, and approximately 140m northeast side of this slope failure. The spring of northeast side of this slope failure is seepage from the drainage channel.

Fig.4 shows the topography of the source areas of debris flow at the B, C tributary Tobinosu torrent. The average slope angle of this area is 35° which is a bit of steeper than the Taishi-do area. In this area, there are 3 slope failures triggered debris flows due to heavy rainfall. The slope failure at the B tributary locates in torrent bed whose volume is 2500m<sup>3</sup>. At the C tributary, there is large type slope failure (called large slope failure at the C tributary) and a small slope type slope failure (called small slope failure at the C tributary), with a total volume of 3500m<sup>3</sup>(Hiramatsu et al., 1999). Depth of these slope failures is 2-3m. In addition, there is the old slope failure with a volume of hundreds located between the slope failure at the B tributary and the large slope failure at the C tributary. Also, there are some small recent and old slope failures illustrated in the northeast part of this figure. These small failures are not considered in this study because volume is very small and surface layer is thin. There are four springs at this area, located in the C tributary. One is on the scarp of the large slope failure at the C tributary. The others are located on the scarp of the small slope failure and at the upper slope of this slope failure.

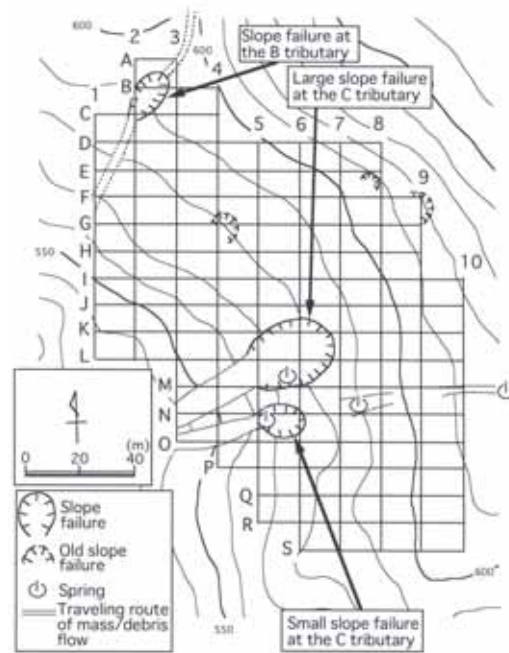


Fig. 4 Measurement net of the B, C tributaries at Tobinosu torrent

### 3. Methodology of the investigation and stability analysis

#### 3.1 One-meter depth underground temperature survey

Takeuchi (1980, 1981) developed the one-meter depth underground temperature survey for detecting the subsurface groundwater flow at natural slope and leakage of water at the river embankment. The principle of this survey is that the difference in a relative underground temperature disturbed by vein of groundwater is measured at a depth of 1m. The appropriate time for this survey in Japan is summer and winter when a difference in temperature between flowing groundwater and surface is large. We carried out the one-meter depth underground temperature survey at the Taishi-do area on September 2000 and at the B, C tributaries Tobinosu torrent on September 2001. The stages of this survey are as follows:

- 1) 10m x 15m mesh of measurement point is set up in the surveying area. Measurement points at the Taishi-do area are 259 and the B, C tributaries at Tobinosu torrent are 139 (shown in Fig. 2 and 3). There are no measurement points in the northeast and southwest parts in Fig. 3. In these parts the surface layer is less than 1m (bedrock is partly exposed), therefore the one-meter depth underground temperature survey couldn't be carried out.
- 2) The hole of 1m at these points are dug by steel pick ( = 2.5cm, ℓ=150cm) and hammer (3kg).
- 3) Precision type thermometer (readable precision is 0.01°C) inserts until the bottom of these holes.

- 4) Measurement of the depth of 1m is after 10 minutes from insertion of the thermometer.

### 3.2 Water quality measurement

Measurement points of water quality investigation in and around the one-meter depth underground temperature surveying areas were at the three springs in Taishi-do area shown in Fig. 2 and the four springs at the B, C tributaries in Tobinosu torrent shown in Fig. 3. In order to know the origin of groundwater, there is necessity to obtain the chemistry ingredient of the deep groundwater in a slope such as the groundwater in boreholes. Therefore, we measured the quality of water in boreholes and from the spring at torrent bed (underflow) at the Z6 block when the One-meter depth underground temperature surveys at these areas were carried out. These boreholes and the spring are shown in Fig. 2. In this figure, The BV5-12, B14, B16 are type of non-strainer up to the bottom of boreholes (slip surface). The DB-T is drainage borehole and the end of it has reached bedrock. The measured items at the B, C tributaries in Tobinosu torrent and the Z6 block are water temperature and electric conductivity. Chemical analysis is carried out at the some measurement points in these areas. The analyzed items in this study are  $\text{Na}^+$ ,  $\text{K}^+$ ,  $\text{Ca}^{2+}$ ,  $\text{Mg}^{2+}$ ,  $\text{Cl}^-$ ,  $\text{HCO}_3^-$ , and  $\text{SO}_4^{2-}$ . At the Taishi-do area, only water temperature is measured because of the low discharge from springs.

### 3.3 Calculate of maximum slope angle and stability

In this study, Maximum slope angle is calculated as follows. First, four points (measurement points for the one-meter depth underground temperature survey) formed on the intersection of adjacent measurement net (10m x 15m) are defined as one grid. The reason for using measurement points of the one-meter depth underground temperature survey is for comparison between the result of slope angles (safety factor) and the result of this survey. Next, any three points are chosen among these four points, and the steepest angle is geometrically calculated in the portion of the shape of triangle surrounded by these three points. This calculation is carried out for all the combinations in a grid, and the maximum value is the maximum slope angle of a grid among these results.

Estimation of slope stability at the Taishi-do area and at the B, C tributaries in Tobinosu torrent was performed using the formula of infinite slope. This formula is as follow:

$$F_s = \frac{c' + \{\gamma' h_w + (\gamma_{sat} - \gamma_w)(H - h_w)\} \cos^2 \beta \tan \phi'}{\{\gamma' h_w + \gamma_{sat}(H - h_w)\} \cos \beta \sin \beta} \quad (1)$$

where  $c'$ : cohesion in terms of effective stress,  $\phi'$ :

friction angle in terms of effective stress,  $\gamma_t$ : moist unit weight,  $\gamma_w$ : unit weight of water,  $\gamma_{sat}$ : saturated unit weight,  $H$ : depth of mass,  $h_w$ : location of groundwater level in the mass (Facing down is made positive),  $\beta$ : slope angle.

The value of the parameters used in this calculations are  $\gamma_t = \gamma_{sat} = 18.1 \text{ kN/m}^3$ ,  $\gamma_w = 9.81 \text{ kN/m}^3$ ,  $c' = 0 \text{ kPa}$ ,  $\phi' = 38.0^\circ$ , and  $H = 2.0 \text{ m}$ .  $c'$  and  $\phi'$  were obtained from the ring shear tests which Fukuoka (1991) carried out on the colluvium material of the Zentoku landslide. In addition,  $\beta$  is the maximum slope angle of each grid.

## 4. Investigation and analysis results

### 4.1 Distribution of slope angle and slope failures

Fig.5 shows a distribution of maximum slope angle at the Taishi-do area. In this figure, the slope angle is divided into three categories: less than  $30^\circ$ , more than  $30^\circ$  to less than  $40^\circ$ , and more than  $40^\circ$ . Although the slope greater than  $30^\circ$  distribute almost uniformly across the measurement net, the east part of the measurement net shows a higher concentration. The slopes greater than  $40^\circ$  are distributed mostly at southeast and a part of northeast. The slope failures at F16, F17 and K13 are located in the area of gradients greater than  $40^\circ$ . On the other hand, the slope failure at Taishi-do fall within the category of gentle slopes less than  $30^\circ$ .

Fig.6 shows a distribution of the maximum slope angle at the area of B, C tributaries in Tobinosu torrent. The classification of slope angles is the same as in Fig.5. In this area, the slopes less than  $30^\circ$  are

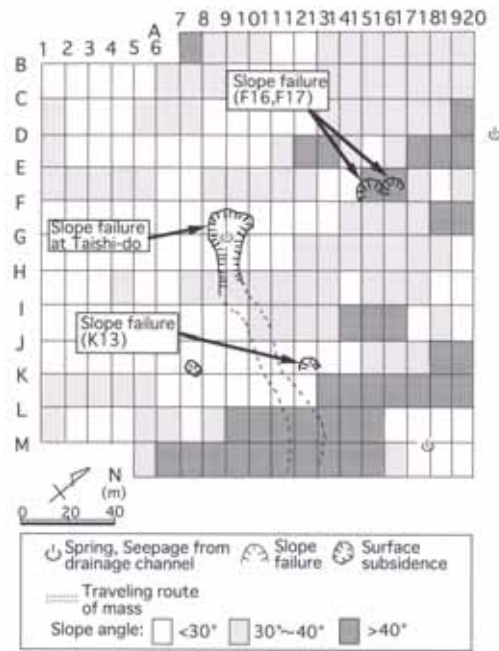


Fig. 5 Distribution of maximum slope angle at the Taishi-do area

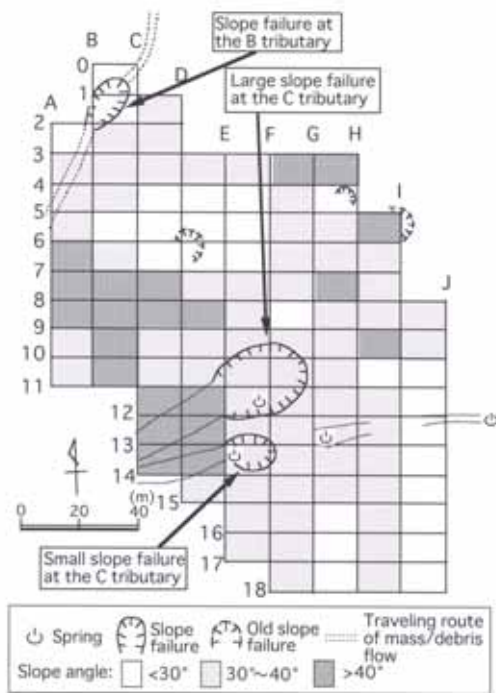


Fig. 6 Distribution of maximum slope angle at the B, C tributaries at Tobinosu torrent

concentrated at southeast and northwest. In addition the slopes greater than  $40^\circ$  are distributed at northeast and southwest in the measurement net. These parts are nearby the thin part of surface layer mentioned above. The large and small slope failures locate within the area with slopes greater than  $30^\circ$ . However, the slope failure at the B tributary and old slope failure locate on gentle slope less than  $30^\circ$ , which is the same as the case of the Taishi-do area. Then, we estimate stability of each grid at these areas by using the slope angle in Fig. 5 and Fig. 6 under a formula (1).

Fig. 7 shows the result in the case when pore water pressure value is equivalent to 0.5m of the groundwater level from slip surface and 1.0m (extreme condition) from this. In this figure, the slopes with  $F_s \leq 1$  for the water level at 0.5m occupy approximately 40 percent of the measurement net. Furthermore, the slopes showing  $F_s \leq 1$  for the water level at 1.0m occupy approximately 60 percent at that in the Taishi-do area. Although the members of potential slope failures estimated by calculation are significantly greater than the actual member of failures, three slope failures where are F16, F17 and K13 located in the area with  $F_s \leq 1$  for the water level at 1m. The slope failure at Taishi-do locates in  $F_s > 1$ , in other ward, locates in stable slope under each pore water pressure condition against to other slope failures.

Fig. 8 shows the result of stability analysis under same pore water condition as in Fig. 7. The case of the B, C tributaries in the Tobinosu area is that the slopes with  $F_s \leq 1$  for the water level at 0.5m occupies approximately half of the area of the measurement

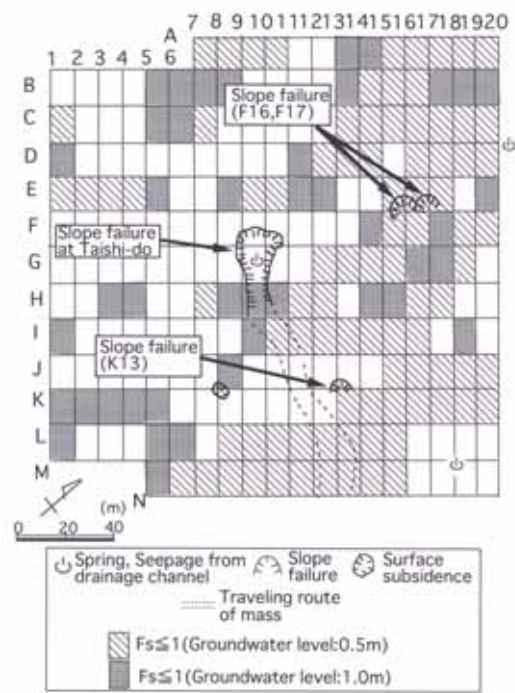


Fig. 7 Distribution of safety factors at the Taishi-do area

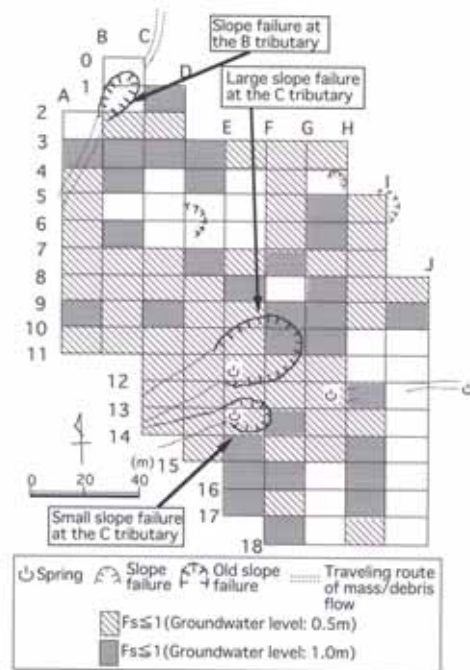


Fig. 8 Distribution of safety factors at the B, C tributaries at Tobinosu torrent

net, and for a water level at 1.0m occupies approximately 80 percent of the measurement net. The large and small slope failures at the C tributary locate in the area of  $F_s \leq 1$  for the water level at 1m. However, the slope failure at the B tributary and the old slope failure around D6 measurement point occurred within the area of  $F_s > 1$ , which is similar

with the result of Taishi-do area shown in Fig.7.

#### 4.2 Distribution of underground temperature

The value of measured temperature at a depth of 1m is affected by factors, i.e., annual variation of ground temperature during survey period, ground conditions, and geological condition etc. We carried out a statistical analysis of measured data to calculate the correction values for the annual variation of ground temperature during survey period. Ground conditions weren't corrected because the material in these surveying areas didn't differ significantly (Furuya et al., 2000 and Furuya et al., 2001).

Fig.9 shows the isothermal diagram of correction values from 12 to 22°C by 1°C at the Taishi-do area. Maximum ground temperature is 21.0°C (B6), minimum ground temperature is 12.3°C (F17), and average ground temperature is 18.2°C within this area. In this figure, the eastern part of the measurement net shows an underground temperature below the average. On the other hand, the underground temperatures in western part are higher than the average. There are three large zones with temperatures less than 18°C (i.e. slightly less than average value) at the Taishi-do area: 1) From C1 and C3 to G9 (E6 is a bit high value) which is approximately the direction from east to west, 2) From E17 to N15 through L12 direction which is approximately oriented on southeast northwest, and 3) From A17 and A19 to D20 located at north part of the measurement net. All slope failures at the Taishi-do area locate in the zone of temperatures less than 18 °C. The temperature of the slope failure at Taishi-do and K13 are a little lower than average underground temperature. However, the slope

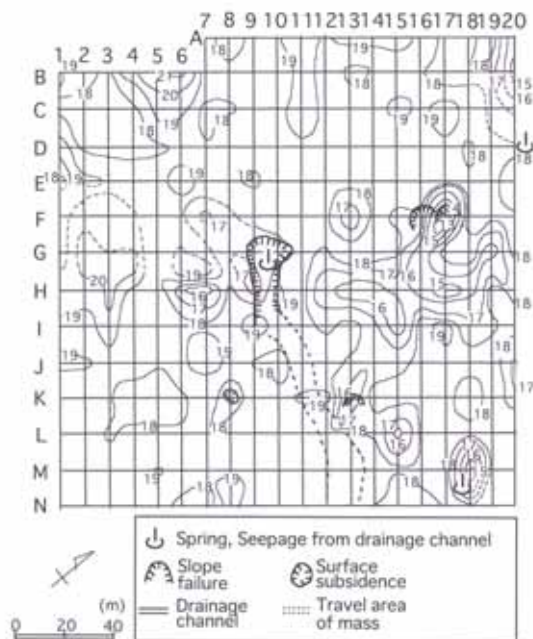


Fig. 9 Isothermal diagram at the Taishi-do area

failures at F16 and F17 locate within the low temperature zone. The slope failure at F17 is also in the zone of the minimum underground temperature. This is a characteristic fact in the Taishi-do area.

Fig.10 shows the isothermal diagram of correction values of the one-meter depth underground temperature survey and local temperature around springs at the B, C tributary in Tobinosu torrent from 15.5 to 20.5°C by 1°C. Maximum ground temperature is 20.6°C (A3), minimum ground temperature is 15.1°C (E13), and average ground temperature is 18.9°C at this area. Groundwater temperature at springs in the B, C tributaries at the Tobinosu torrent are lower than minimum measurement value. The temperature at upper J12 is 12.7 °C; in point F12 (the large slope failure at the C tributary) is 13.9°C; at G12-13 is 14.1°C, and at E13 (the small slope failure at the C tributary) is 13.5°C.

#### 4.3 Water quality for springs and boreholes

Table 1 shows measurement results of groundwater temperature at springs at the Taishi-do area and in boreholes at the Z6 block during the one-meter depth underground temperature survey in the Taishi-do area. The groundwater temperature at the spring of the Taishi-do slope failure was found to be higher than the values measured at another springs and boreholes. For instance, the groundwater temperature of the slope failure at Taishi-do is 2.9 to 4.0°C higher than springs near the D20 and M18 of the measurement net. Groundwater temperature in boreholes at Z6 block is ranging from 11.8 to 12.8°C, which is almost the same as the underground temperature at a 1m depth in F17 of the measurement net.

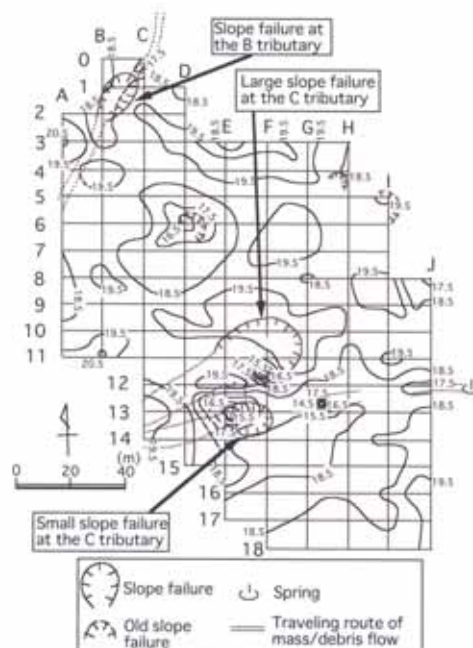


Fig. 10 Isothermal diagram at the B, C tributaries in Tobinosu torrent

Table 1 Groundwater temperature of surveying period at the Taishi-do area

Location	Temp. (°C)	Condition
Slope failure at the Taishi-do	17.8	Spring
Nearby D20	13.8	Seepage from drainage channel
M18	14.9	Spring
Borehole BV5-12	11.8	G.L.77m
Borehole B14	12.6	G.L.70m
Borehole B16	12.8	G.L.49m

Fig. 11 gives as the results of measured groundwater temperature, electric conductivity and hexa diagram of the ion concentrations at some springs of the C tributary at the Tobinosu torrent, as well as at the boreholes and underflow in the Z6 block during the one-meter depth underground temperature survey. In this figure, the measured groundwater temperature at the springs in the C tributary Tobinosu torrent are approximately the same as the values measured in all points of Z6 block (i.e., 12 to 14°C). When attention is paid to the results of electric conductivity, the springs at the C tributary have the values in two diagrams (Upper J12 and G12-13) the same as the results of boreholes in the Z6 block, and the value in third diagram (Side of F12: Large slope failure at the C tributary) the same as

the data of TB-K (Underflow) at the Z6 block. From the results of hexa diagram, the Upper J12 and G12-13 don't show a clear water quality pattern. This is similar with the analysis results at TB-K at the Z6 block. On the other hand, the Side of F12 has clear Ca-HCO<sub>3</sub> water quality type, which is the same as in points B16 and the DB-T of the Z6 block. This water quality type has the same tendency as the results provided by Yoshioka et al., (1973) who carried out investigation along the Iya River. The water quality at BV5-12 is Na, K-HCO<sub>3</sub> type, which is different from the water quality at another boreholes in the Z6 block. The reason for this difference may be the fact that the geology of the upper part of slope is different from the geology of middle part of slope at the Z6 block shown in Fig.2.

## 5. Relationship between location of slope failures and veins of groundwater

### 5.1 Case of the Taishi-do area

As mentioned before, the principle of the one-meter depth underground temperature survey is measuring the disturbance of underground temperature due to groundwater flowing in water veins. We suggest that veins of groundwater affect zones slightly lower than average underground temperature. Fig. 12 shows the coupled distributions of the low underground temperature zones, veins of groundwater, the real slope failures and the slopes with  $F_s \leq 1$  for a groundwater level at 50cm above slip surface at the Taishi-do area. The low underground temperature zones are divided

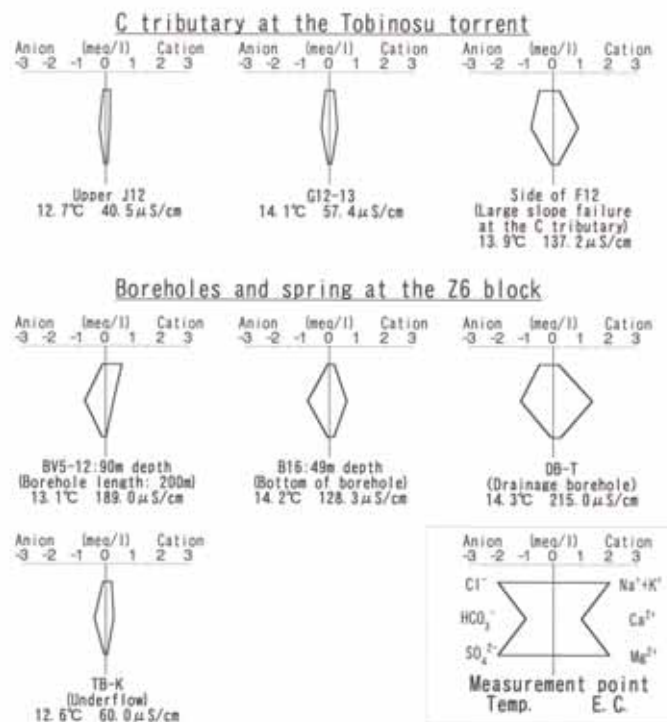


Fig. 11 Results of water quality analysis

into lower than average underground temperature zones (18.2°C) and zones with temperatures lower by 2°C than average underground temperature. There are five veins of groundwater at the Taishi-do area (Furuya et al., 2004): Zone 1 from C1 and C3 to G9, Zone 2 from E17 to N15 through K13, Zone 3 from A17 and A19 to D20, Zone 4 area around H7, and Zone 5 area around M18. Zone 1 and 2 are large veins of groundwater for the measurement net, however, the groundwater type is different in these two veins represent. In zone 1 the lowest value is 16.9°C at point H9 (Furuya et al., 2000) and the spring in slope failure at Taishi-do is 17.8°C as shown in Table 1. Thus the temperature in this vein is not so low compared with the average value, and is 4 to 5°C higher than the boreholes at the Z6 block. On the other hand, the lowest ground temperature at a depth of 1m in zone 2 is 12.3°C at point F17. This is also the lowest value in the measurement net, and is approximately equal to the groundwater temperature at the boreholes of Z6 block. In addition, when the ground temperature of F17 was measured, groundwater was oozing through the measurement hole of this measurement point (Furuya et al., 2000). Therefore, it may be stated that the vein of groundwater in zone 1 is of shallow origin, while the vein of groundwater in zone 2 originates groundwater from deep layers. The other veins of groundwater in the surveying area aren't widely distributed being rather than local. However, they have remarkable low underground temperature part. This may be attributed to the small scale of these veins rising from deep layers.

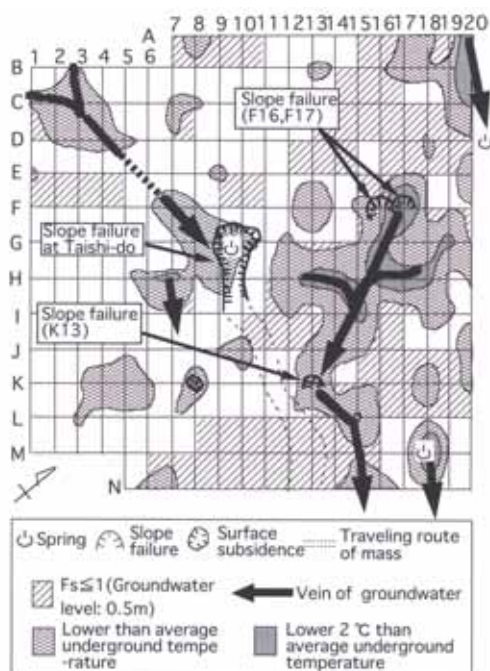


Fig.12 Distribution of veins of groundwater, safety factors, and slope failures at the Taishi-do area

The slope failure at associated with  $F_s > 1$  in Fig. 5 (gentle slope less than 30°) is actually locates on the vein of groundwater corresponding to zone 1. Furthermore, the results of stability analysis indicate a stable slope even for a pore water pressure calculated from a groundwater level at 1.0m above the slip surface. Hence, it may be concluded that the slope failure at Taishi-do was caused by the increase in pore water pressure due to concentrated groundwater along the vein of groundwater in zone 1 during the heavy rainfall. The slope failures at F16 and F17 locate on and nearby the beginning of the vein of groundwater in zone 2. Recall that underground temperature at a 1m depth in point F17 is lowest, and is approximately equal to the groundwater temperature in the boreholes at the Z6 block. Thus we can consider as the outlet of groundwater originating from the deep layers. In these circumstances the occurrence of these slope failures could be related to the existence of a vein of groundwater originating from the deep layers. This vein of groundwater is flowing like underflow in subsurface toward K13. The vein of groundwater in zone 2 could also be responsible of the slope failure at K13.

### 5.2 Case of the B, C tributaries at Tobinosu torrent

Fig. 13 shows the coupled distributions of the low underground temperature zones, veins of groundwater, the real slope failures and the slope with  $F_s \leq 1$  at the B, C tributaries, Tobinosu torrent. The assumed water level for slope stability calculation was at 50cm

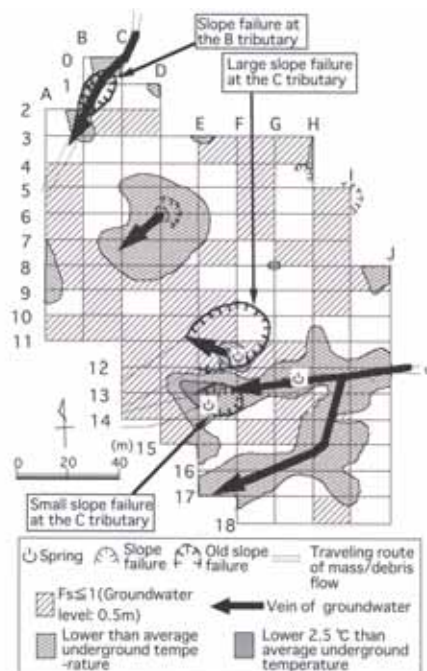


Fig.13 Distribution of veins of groundwater, safety factors, and slope failures at the B, C tributaries in Tobinosu torrent



above the slip surface. This figure shows the lower than average underground temperature zones (i.e., 18.2°C) and zones with temperatures lower by 2.5°C than average underground temperature. The veins of groundwater are as follows: zone 1 along the B tributary (C0 to B3); zone 2 large slope failure at the C tributary; zone 3 upper slope of J12 to the small failure at the C tributary with branch vein at I11 to F17, and zone 4 the area within a range of approximate 40m x 40m around D6 (Furuya et al., 2001). The vein of groundwater in zone 3 is underflow type because the springs in the upper slope of the small slope failure at the C tributary are distributed over a line and these springs show a concentration of dissolved ions (electric conductivity) similar with the TB-K at the Z6 block (see the results of water quality analysis in Fig. 11). The branch stream of this vein of groundwater starting from I12 may also be of underflow type. No spring exists at the B tributary. However, it is believed that the vein of groundwater along the B tributary is flowing under the torrent bed of this tributary because the zone of low underground temperature is along the torrent bed. Hence, it can be concluded that the underflow type is the same as for TB-K at Z6 block. The low temperature distribution disappears around B3 suggesting that the vein of groundwater infiltrates into the deep zone of the torrent bed. The large slope failure at the C tributary has a spring on the lateral side at F12, which scale of vein is very small. The water quality type of this spring differs from that of the vein of groundwater in zone 3 which flows neighboring the large slope failure shown in Fig. 11. In the Zentoku area, many cracks were found on outcrops of bedrock during field investigations, as well as in the rock mass during the construction of a drainage well. Hence, the vein of groundwater in zone 2 appears to be of fissure water type. This vein of groundwater is presumed that raising steep angle from deep layers by the calculation results based on thermal conductivity type differential equation (Furuya et al., 2001). The water quality of this vein and the dissolved ion concentration are the same as at locations B14 and DB-T in Z6 block. Therefore, the vein of groundwater zone 2 is discharging from the deep layers equivalent to the slip surface at Z6 block. There is no spring around D6. However, it is believed that the deep layer of groundwater is rising nearby surface because the zone of underground temperatures lower by 2.5°C than the average is located around D6.

There are three slope failures generating debris flows in the analyzed measurement net. The common feature in these slope failures is that they occurred in the zones of low underground temperature. Among these, the slope failure at the B tributary and the small slope failure at the C tributary are related to the underflow type vein of groundwater. On the other

hand, the large slope failure at the C tributary is related to the fissure water type vein. However, it is presumed that this slope failure rather develops retrogressively towards the upper slope instead of occurring at once. There is an old slope failure at D6 that could have been caused by water rising from fissures. This study demonstrated that by coupling the results of stability analysis with the distribution of veins of groundwater within the analyzed domain, it is possible to narrow the regions associated with a high potential of slope failure.

In Figs. 12 and 13, it is clearly shown that slope failures are located on and around the veins groundwater at the landslide in crystalline schist area. These veins are divided into flowing shallow layer and flowing origination from the deep layers. The vein of groundwater originating from deep layers is at least of two types based on the analysis results of the water quality. The first type correspond to the infiltration of rainfall into the deep layers of slope; in this case the groundwater temperature becomes approximately the same as the temperature of the surrounding material, and this discharges to the surface in a short time. The second type is representative for the groundwater is stored for a certain amount of time, and subsequently discharged to the surface when the water chemistry the dissolved substance from rock or colluvium material. In both cases, Figs. 12 and 13 suggest that it is of great importance to obtain the detailed information about veins of groundwater. This information combined with the results of slope stability analysis would present in more accurate assessments of the slope failure risk in the investigation area.

## 6. Conclusions

One-meter depth underground temperature survey was carried out in addition to the stability analysis, and the water quality investigation to clarify the relationship between the distribution of real slope failures and the distribution of veins of groundwater in a landslide in prone area in crystalline schist. The conclusions of this investigation may be summarized as follows:

- 1) The real slope failures locate around the vein of groundwater or in the zones considered as the veins of groundwater rising from deep layers.
- 2) The vein of groundwater originating from deep layers origin is at least of two types. The first type is associated with the groundwater infiltrating from rainfall, which has approximately the same temperature as the surrounding material, and is discharged to the surface in short time. The second type corresponds to the infiltrated groundwater stored for during a certain amount of time, followed by subsequent discharge to surface including the dissolved substance from rock or colluvium material.

## Acknowledgments

We wish to thank Dr. A. Takeuchi, Associate Prof. H. Fukuoka, Dr. A. Trandafir (Disaster Prevention Research Institute, Kyoto University), Prof. of former O. Sato, Prof. H. Marui, and Dr. N. Watanabe (Research Institute for Hazards in Snowy Areas, Niigata University) for their helpful suggestions.

## References

- Hiramatsu, S., Ishikawa, Y., Osanai, N., and Miyoshi, I. (1999): Report of sediment-related disaster on June 29, 1999 in Nishiiyayama village Tokushima Prefecture, Japan (Prompt Report), *Jour. of the Japan Society of Erosion Control Engineering*, Vol.52, No.3, pp.44-49.
- Fukuoka, H. (1991): Variation of the friction angle of granular materials in the high-speed high-stress ring shear apparatus –Influence of re-orientation, alignment and crushing of grains during shear-, *Bulletin of the Disaster Prevention Research Institute, Kyoto University*, Vol. 41, Part 4, No. 362, pp.243-279.
- Furuya, G., Sassa, K., Hiura, H., and Fukuoka, H. (1999): Mechanism of creep movement caused by landslide activity and underground erosion in crystalline schist, Shikoku Island, southwestern Japan, *Engineering Geology*, Vol. 53, pp.311-325.
- Furuya, G., Suemine, A., Osanai, N., and Hara, R. (2000): Distribution of slope failures caused by heavy rain on 29 June 1999 and groundwater vein-streams in Taishido, Zentoku landslide, Shikoku Island, Japan, *Annual Report of Research Institute for Hazards in Snowy Areas, Niigata University*, No. 22, pp.44-60.
- Furuya, G., Suemine, A., Osanai, N., Hara, R., Sato, O., and Komatsubara, T. (2001): Detecting of groundwater flow at source area of debris flow in crystalline schist mountains, *Annual Report of Research Institute for Hazards in Snowy Areas, Niigata University*, No. 23, pp.35-44.
- Furuya, G., Suemine, A., Hiura, H., Fukuoka, H., Sassa, K., and Marui, H. (2004): Veins of groundwater flow relating to slope failures in layer of colluvium at crystalline schist area, *Jour. of the Japan Landslide Society*, Vol. 40, No.6, pp.472-483.
- Kaibori, M. (1986): Study on the movement of the slope failure materials, Doctor thesis of Graduate school of Agriculture, Kyoto University, p.99.
- Okimura, T., and Nakagawa, M. (1988): A method for predicting surface mountain slope failure by a digital landform model, *Jour. of the Japan Society of Erosion Control Engineering*, Vol.41, No.1, pp.48-56.
- Okimura, T., and Nakagawa, M. (1989): A wide using method for predicting probable failure of surface by the index of a geomorphic driving force, *Jour. of the Japan Society of Erosion Control Engineering*, Vol.41, No.6, pp.14-21.
- Takeuchi, A. (1980): Method of investigating groundwater-vein-streams by measuring one-meter-depth in landslide areas (I), *Jour. of Japanese Association of Groundwater hydrology*, Vol. 22, No.2, pp.11-39.
- Takeuchi, A. (1981): Method of investigating groundwater-vein-streams by measuring one-meter-depth in landslide areas (II), *Jour. of Japanese Association of Groundwater hydrology*, Vol. 23, No.1, pp.1-27.
- Tanaka, S. (1985): Relation between heavy rain and slope failure, Bulletin of Reclamation Engineering Research Institute, Faculty of Engineering, Kobe University, Vol.3, pp.1-22.
- Tsukamoto, Y., Hiramatsu, S., and Shinohara, S. (1973): Study on the growth of stream channel (III) – Relationship between 0 (zero) order channels and landslides-, *Jour. of the Japan Society of Erosion Control Engineering*, Vol.26, No.2, pp.14-20.
- Yoshioka, R., and Furuya, T. (1973): Studies on the water quality of geologically different landslide, *Disaster Prevention Research Institute Annuals, Kyoto University*, No.16B, pp.127-13

## 要 旨

結晶片岩の地すべり地において、地温探査、安定解析および水質分析結果から斜面崩壊と地下水脈の分布の関係について検討した。その結果、崩壊発生箇所は地下水脈の分布に関連すること、この水脈は浅部のみを流れる地下水、山体内での貯留時間が短い深部地下水、この時間が長い深部地下水であることが判明した。また、安定解析結果と水脈分布情報を併用したところ、崩壊危険斜面をある程度絞り込めることが示唆された。

**キーワード:** 豪雨, 崩壊分布, 1 m深地温探査, 安定解析, 水質分析

## 結晶片岩地すべり地における地下水脈・傾斜分布と崩壊箇所との関係

○古谷 元・佐々恭二・末峯 章

## 1. はじめに

四国の三波川結晶片岩帯の山岳地域は日本の代表的な地すべり多発地域であるが、豪雨がトリガーになった流動性の斜面崩壊も頻繁に発生している。斜面崩壊は斜面の傾斜角が $30\sim 60^\circ$ の間で発生し易く、この角度が危険斜面の目安とされる場合が多い。結晶片岩の山岳地域ではこのような比較的急傾斜の角度を有する斜面が数多いが、豪雨後に現地踏査を行うと崩壊が発生した箇所は極めて少ない。豪雨時の斜面崩壊において最も支配的な因子は間隙水圧である。本報では地下水に関する計測情報が比較的入手しやすい地すべり地を対象とし、地下水脈、最大傾斜分布と斜面崩壊の発生箇所との関係について検討する。

## 2. 調査対象地域および検討の概要

調査対象地域は、1999年6月29日の集中豪雨による流動性の崩壊が発生した徳島県西祖谷山村の善徳地すべり地 Z6 ブロックの大師堂周辺ととびのす谷源頭部である。流動地下水の平面分布状況は1m深地温探査（測点間隔：10m×15m）と水質調査の結果により推定した。斜面傾斜角の分布は、1:1,000の地形図上に記載した1m深地温探査の測点網において隣り合う測点で矩形状に囲まれる範囲（セル）を決め、セル内の最大傾斜角で表した。各セルにおける安全率は長大斜面における算定式で算出した。この計算では崩壊土層深は2m、 $\gamma_t$ は $1.85\text{tf/m}^3$ 、強度定数はリングせん断試験によるピーク強度（ $c=0$ 、 $\phi=38.0^\circ$ ）を用いた。

## 3. 結果と考察

2箇所の調査対象地域において検討したところ、以下の知見を得た。なお、本報では紙面の都合上、大師堂周辺で発生した斜面崩壊と流動地下水脈の位置、およびすべり面上の水位が0.5mに相当する間隙水圧で安全率 $F_s$  1.0になる箇所を示した図のみを載せている。

これらの調査対象地域の平均傾斜角は $32\sim 34^\circ$ である。斜面崩壊は従来から指摘されている遷移点（遷急点、遷緩点）周辺で発生しているが、図に示すように、すべり面上の間

隙水圧が同条件のもとで計算した結果において他の箇所（セル）よりも安定性が高いと評価される緩傾斜（ $20\sim 27^\circ$ ）の箇所でも発生している。流動地下水脈の分布に着目すると、調査対象地域では流動地下水の分布の有無による斜面傾斜角の違いはほとんど無い。斜面崩壊は土層深が著しく薄い箇所を除いて地下水脈の経路付近や斜面内部の地下水が地表面（付近）に流出する箇所が発生する傾向が高い。これは地下水が集中し易い箇所でも斜面崩壊が発生し易いことを示唆する。なお、調査対象地域における斜面内部から流出する地下水は、水質調査結果よりすべり面相当深度のものであった。以上より、結晶片岩の地すべり地で豪雨時に発生する斜面崩壊の危険度を評価するには斜面傾斜角に着目した評価だけでは不十分であり、現地の流動地下水の情報も併用する必要があると考えられる。

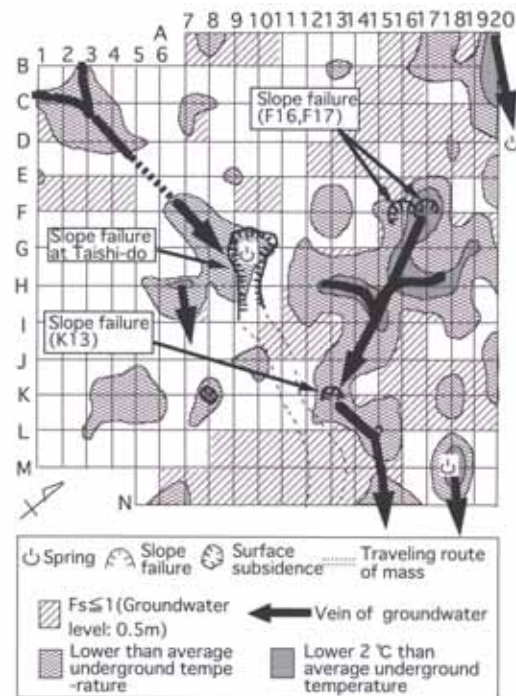


図 大師堂周辺における崩壊発生箇所、流動地下水脈および安全率1以下の分布